IL NUOVO CIMENTO Vol. 29 C, N. 5 Settembre-Ottobre 2006
DOI 10.1393/ncc/i2006-10014-2

Higher-order elastic properties of single crystalline corundum(*)

Jung Mo Lee(1), Chang-Eob Baag(2) and Sang Gyu Jo(3)

(1) *Department of Geology, Kyungpook National University - Daegu 702-701, Korea*
(2) *Department of Geological Sciences, Seoul National University - Seoul 151-742, Korea*
(3) *Department of Physics, Kyungpook National University - Daegu 702-701, Korea*

(ricevuto il 20 Aprile 2006; approvato il 21 Luglio 2006)

Summary. — Corundum is frequently used for high-pressure and high-temperature applications. Its second-order pressure derivatives are, however, not measurable. A static rigid-ion lattice model for corundum, utilizing exponential-type repulsive force, is developed. The lattice parameters are determined from measured data of the bulk modulus and C_{33}. Using these lattice parameters first-order pressure derivatives of bulk modulus and C_{33} are computed and compared to measured values, respectively. The deviations do not exceed 33%. The second-order pressure derivatives of bulk modulus and C_{33} are predicted and the results come out positive. These are usually negative for oxide mineral of cubic structure.

PACS 91.90.+p – Other topics in solid Earth physics.

1. – Introduction

Corundum is an oxide mineral of rhombohedral structure. It is chemically stable under atmospheric conditions and is frequently used for high-temperature and high-strength applications, for instance as a pressure indicator. In addition, the elastic properties of oxide minerals are of geophysical interest in connection with the composition and the pressure state of the mantle. The structure of corundum has been analyzed [1, 2] and its elastic moduli and their first-order pressure derivatives have been measured [3]. The high-pressure application, however, implies a great deal of uncertainty because corundum is one of the minerals whose second-order pressure derivatives of elastic moduli cannot be measured due to their high stiffness. In this paper, strain nearest-neighbor separation is modeled using the crystal structure. Utilizing the thermodynamic definition of elastic moduli, the lattice parameters are determined, and the first-order pressure derivatives of elastic properties are computed and compared to the measured values. The second-order pressure derivatives of elastic moduli are predicted based on foregoing works.

(*) The authors of this paper have agreed to not receive the proofs for correction.

TABLE I. – *Crystallographic data for corundum: Notations are explained in fig. 1.*

	Pauling and Hendricks [1]	Newnham and Haan [2]
a_H	4.7507 Å	4.7589 ± 0.001 Å
c_H	12.969 Å[(a)]	12.991 ± 0.005 Å
a	5.12 ± 0.01 Å	5.128 Å[(a)]
α	$55°17'$	$55°17'$[(a)]
Interatomic	B or C to A : 1.990 ± 0.020	$R_1 - O_1$: 1.97 ± 0.015
distance	D or E to A : 1.845 ± 0.015	$R_1 - O_5$: 1.86 ± 0.010
in	B to C : 2.74 ± 0.03	$R_1 - R_3$: 2.79 ± 0.002
Å	2.495 ± 0.025	$O_1 - O_2$: 2.52 ± 0.002

[(a)] denotes that the values are computed using the relationship between rhombohedral and hexagonal unit cells for comparison.

2. – The crystal structure of corundum

The crystal structure of corundum, α-Al_2O_3 was analyzed by Pauling and Hendricks [1] using X-ray reflection data and refined by Newnham and de Haan [2] using a least-square analysis of single-crystal X-ray data. Corundum exhibits a rhombohedral structure, each aluminum cation being coordinated by six oxygen anions at the corners

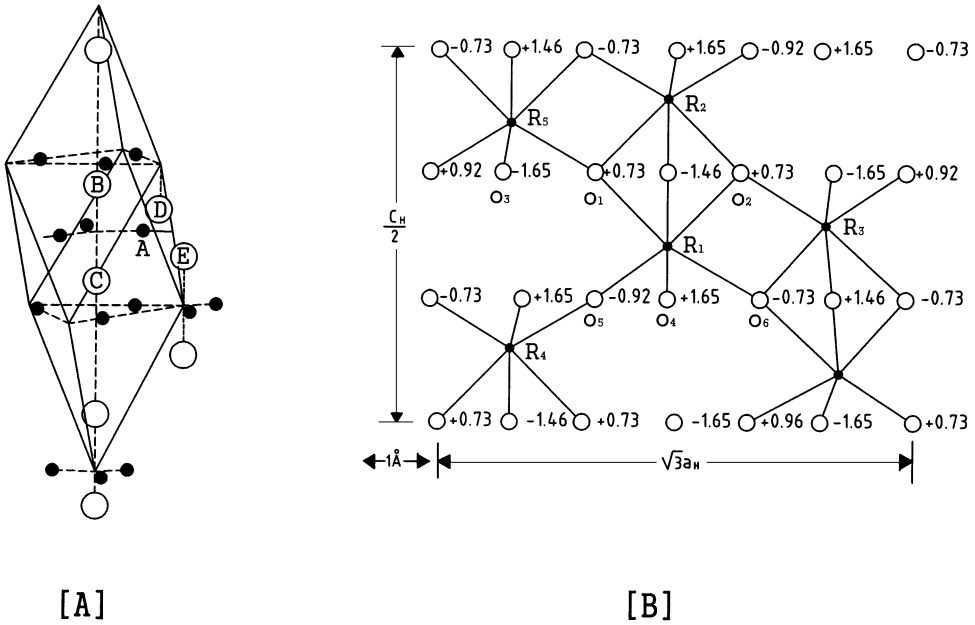

Fig. 1. – [A] The arrangement of atoms in the rhombohedral units of corundum; small solid circles represent oxygen atoms, while large open ones do aluminum atoms (after Pauling and Hendricks [1]). [B] Projection of corundum on $(2\ \bar{1}\ \bar{1}\ 0)$; the vertical distances from the oxygen ions to the plane of the projection are given in Å, while the aluminum ions lie in the projection plane (after Newnham and de Haan [2]).

TABLE II. – *Zero pressure values of second-order adiabatic elastic constants (in* $10^{11}\mathrm{dyne/cm^2}$*) and of their isothermal pressure derivatives of crystalline corundum* ($C_{12} = C_{11} - 2C_{66}$).

$\mu\nu$	11	12	13	14	33	44	66	K_V^s
$C_{\mu\nu}^s$	49.76	16.26	11.72	−2.29	50.19	14.72	16.75	25.42
$(\partial C_{\mu\nu}^s/\partial p)_T$	6.17	3.28	3.65	0.13	5.00	2.24	1.45	4.32

of a distorted octahedron. Three of these oxygen atoms are a few percent closer to the aluminum atom than the other three. Each oxygen atom is surrounded by four aluminum atoms, two of which are nearer than the other two. The smallest rhombohedral unit has $a = 5.12 \pm 0.01$ Å and $\alpha = 55°17'$, and contains two Al_2O_3 [1]. The oxygen atom arrangement can be approximately taken as a hexagonal close packing, with trivalent cations occupying two thirds of the octahedral interstices. The conventional hexagonal unit cell, right prism with rhombus base, contains six Al_2O_3 and has $c_H = 12.991 \pm 0.005$ Å and $a_H = 4.7589 \pm 0.001$ Å [2]. The arrangement of atoms in the unit structure of corundum is shown in fig. 1, and the crystallographic data are listed in table I. As shown in fig. 1B the aluminum ions lie alternatively on the plane one-third and two-thirds of the distance between oxygen layers. The crystallographic data for corundum refined by Newnham and de Haan [2] are a little different from those of Pauling and Hendricks [1], and the differences do not exceed the range of uncertainty.

3. – The elastic properties of corundum

Zero pressure values of the second-order adiabatic elastic constants and the isothermal pressure derivatives of single crystalline corundum have been measured by Gieske and Barsch [3]. They compared their results with values previously reported in the literature and pointed out almost no difference. They also calculated the adiabatic bulk modulus and the isothermal pressure derivatives using equations derived by Thurston [4]. Their results are listed in tables II and III, and will be used in this work. Although the corundum structure does not have exact hexagonal symmetry, the deviation from hexagonal symmetry is rather small. This is reflected by the fact that the rhombohedral angle of $55°17'$ deviates only a little from the value $53°30'$ corresponding to the hexagonal close pack structure, and that the elastic constant C_{14} is small [3]. So the elastic property of corundum can be approximated by the transversely isotropic case.

TABLE III. – *The second-order isothermal compliances (in* $10^{-13}\mathrm{cm^2/dyne}$*) and the isothermal pressure derivatives of the second-order thermodynamic adiabatic elastic coefficients* ($S_{12} = S_{11} - (1/2)S_{66}$).

$\mu\nu$	11	12	13	14	33	44	66
$S_{\mu\nu}^T$	2.353	−0.697	−0.383	0.474	2.176	6.939	6.099
$B_{\mu\nu}$	7.740	2.467	2.819	0.101	6.842	3.451	2.636

TABLE IV. – *Lattice parameters for corundum and atomic constants used in this work.*

Symbol	Value	Unit	Source
N	6	.	
V_c	$\frac{\sqrt{3}}{2}a_H^2 c_H = 2.548 \times 10^{-22}$	cm^3	Calculated from Newnham and de Haan [2]
α	1	.	
r_0	1.915×10^{-8}	cm	Average of Newnham and de Haan [2]
A	25.031	.	Schmaeling [5]
e	4.803×10^{-10}	esu	Clark [9]

4. – The lattice energy of corundum

Corundum is an ionic crystal and its lattice energy consists of Coulombic forces between cations and anions, and short-range intrinsic repulsive forces. The potential due to the Coulombic forces per unit cell is

$$U_c = -\frac{\alpha^2 e^2 N A}{r}\,, \tag{1}$$

where α is the largest common factor in the valences of all three ions, e is the unit of electrical charge, N is the number of stoichiometric molecules in the unit cell, A is the Madelung constant depending only on the structure of the crystal, and r is the nearest-neighbor separation in the crystal. The Madelung constant for corundum has been evaluated by Schmaeling [5]. He approximated the actual crystals with the ideal case in which each aluminum ion is equidistant from six oxygen ions. This approximation makes the three adjacent oxygen ions form an equilateral triangle in a plane normal to the line joining the two aluminum ions and midway between them. Then the structure is determined by three independent parameters, the diagonal of rhombohedral faces (a), one-half the length of a body diagonal (c), and the distance between two adjacent aluminum ions (v). By introducing two dimensionless variables, $\gamma = c/a$ and $\omega = v/a$, Schmaeling evaluated the Madelung constant for corundum,

$$\begin{aligned} A = {} & 25.0312 - 5.930(1.312 - \gamma)^2 - 65.250(0.5454 - \omega)^2 + \\ & + 30.70(1.312 - \gamma)(0.5454 - \omega). \end{aligned} \tag{2}$$

The maximum value of A is 25.0312 when $\gamma = 1.312$ and $\omega = 0.5454$. The deviations in the calculated and observed parameters are approximately 5% [6]. The deviation due to equidistance approximation is 3%. In this work, the maximum theoretical Madelung constant, $A = 25.0312$, is employed, and the mean nearest-neighbor separation, $r_0 = (1.97 + 1.86)/2 = 1.915$ Å, is used. Born and Lande [7] first introduced the $(b \cdot r^{-n})$-type potential of the intrinsic repulsive force between two ions. According to the theory of quantum-mechanical interaction (antisymmetric coupling) of the electrons in the two ions, Born and Mayer [8] used the potential, $U_{\mathrm{B}} = b \exp[-r/\rho]$, where b and ρ are lattice parameters. Using this potential with the help of the law of superposition and the equilibrium condition ($\mathrm{d}U/\mathrm{d}r = 0$), the lattice energy at the equilibrium is

$$U(r_0) = N\left\{-\frac{\alpha^2 e^2 A}{r_0} + \frac{\rho \alpha^2 e^2 A}{r_0^2}\right\} = \frac{N\alpha^2 e^2 A}{r_0}\left\{-1 + \frac{\rho}{r_0}\right\}, \tag{3}$$

where r_0 is the equilibrium nearest-neighbor separation. This potential is an extensive quantity (depending on the volume). The intensive potential (independent of the volume), lattice energy density, becomes

$$\phi(r) = \frac{N}{V_c}\left\{-\frac{\alpha^2 e^2 A}{r} + b\exp[-r/\rho]\right\}, \tag{4}$$

where V_c is the volume of unit cell. The lattice parameters and atomic constants to be used in this work are listed in table IV.

5. – The strain energy relation

The strain energy function, ψ, is taken to be the change in the Helmholtz free-energy density due to deformation resulting from applied stresses, since the models in this work relate to adiabatic conditions. Furthermore stresses may be written in terms of strains, ϵ, $\psi(\epsilon) = F(\epsilon) - F(0)$, where F is the Helmholtz free-energy density of the system. Expanding the strain energy in a Taylor series, and using the conditions, $\psi(0) = 0$ and $\frac{\partial\psi}{\partial\epsilon_\mu}\Big|_0 = 0$, we get

$$\psi(\epsilon) = \frac{1}{2}\frac{\partial^2\psi}{\partial\epsilon_\mu\partial\epsilon_\nu}\bigg|_0 \epsilon_\mu\epsilon_\nu + \frac{1}{6}\frac{\partial^3\psi}{\partial\epsilon_\mu\partial\epsilon_\nu\partial\epsilon_\zeta}\bigg|_0 \epsilon_\mu\epsilon_\nu\epsilon_\zeta + \cdots, \tag{5}$$

where the Voight notation is used. The second-order term of eq. (5) follows Hooke's law. By relating the change in strains to the work done by the traction, the coefficients of the second-order term of eq. (5) result in the adiabatic elastic stiffness moduli,

$$C^S_{\mu\nu} = \frac{\partial^2\psi}{\partial\epsilon_\mu\partial\epsilon_\nu}. \tag{6}$$

Since the strain energy is a part of the internal energy, ψ can be replaced by the lattice energy function, ϕ, when only the static deformation is considered,

$$C^S_{\mu\nu} = \frac{\partial^2\phi}{\partial\epsilon_\mu\partial\epsilon_\nu}. \tag{7}$$

6. – Parameterization of strain and pressure

Since the lattice energy function $\phi(r)$ depends only on the nearest-neighbor distance r, it cannot be directly differentiated with respect to strain and/or pressure. The relations between the nearest-neighbor distance and those quantities will be set up using the crystallographic structure and data of corundum discussed previously.

6˙1. *Strain.* – When strain ϵ_1 (ϵ_{xx}) or ϵ_2 (ϵ_{yy}) occurs, the equilateral triangle formed by the three adjacent oxygen ions will be deformed (fig. 2). The line connecting the adjacent aluminum ions (parallel to the z-axis) will move to the circumcenter (the point equidistant from the vertices) of the deformed triangle without stretching or tilting. In

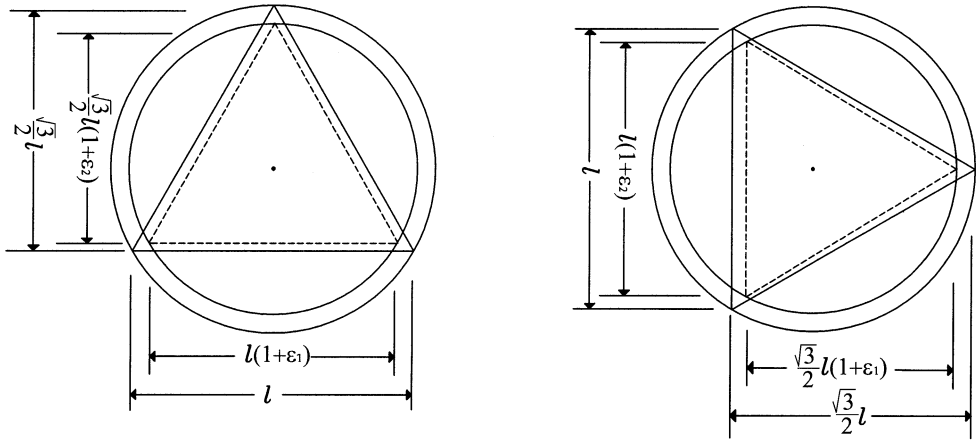

Fig. 2. – Top view of unstrained and strained triangles composed of three adjacent oxygen ions. The aluminum ion is located at the center of the circles. The solid lines denote the unstrained state, while dotted ones do the strained state.

the first case (fig. 2, left), the length of each side in the presence of ϵ_1 becomes, denoting the undeformed length of the side by l,

$$a = l(1+\epsilon_1), \qquad b = c = \frac{l}{2}\sqrt{\epsilon_1^2 + 2\epsilon_1 + 4}, \tag{8}$$

where a is the deformed length of the side parallel to the x-axis. We now add ϵ_2, then a, b, and c become

$$a = l(1+\epsilon_1)\,, \qquad b = c = \frac{l}{2}\sqrt{\epsilon_1^2 + 3\epsilon_2^2 + 2\epsilon_1 + 6\epsilon_2 + 4}. \tag{9}$$

Since the radius of a circle circumscribing the triangle of sides a, b, and c is

$$R = \frac{abc}{4\sqrt{S(S-a)(S-b)(S-c)}}\,, \tag{10}$$

where $S = (1/2)(a+b+c)$, the radius becomes

$$R_{12} = \frac{l}{4}\frac{\epsilon_1^2 + 3\epsilon_2^2 + 2\epsilon_1 + 6\epsilon_2 + 4}{\sqrt{3\epsilon_2^2 + 6\epsilon_2 + 3}}\,. \tag{11}$$

In the second case (fig. 2, right), when the coordinates are rotated by 90°, R_{21} becomes

$$R_{21} = \frac{l}{4}\frac{\epsilon_2^2 + 3\epsilon_1^2 + 2\epsilon_2 + 6\epsilon_1 + 4}{\sqrt{3\epsilon_1^2 + 6\epsilon_1 + 3}}\,. \tag{12}$$

Since changes of the strain energy due to ϵ_1 and ϵ_2 should be the same, we take the average of R_{12} and R_{21}.

$$R = \frac{l}{8}\left(\frac{\epsilon_1^2 + 3\epsilon_2^2 + 2\epsilon_1 + 6\epsilon_2 + 4}{\sqrt{3\epsilon_2^2 + 6\epsilon_2 + 3}} + \frac{\epsilon_2^2 + 3\epsilon_1^2 + 2\epsilon_2 + 6\epsilon_1 + 4}{\sqrt{3\epsilon_1^2 + 6\epsilon_1 + 3}}\right). \tag{13}$$

When ϵ_3 (ϵ_{zz}) occurs, the distance from the triangle to aluminum oxide becomes

$$Z = d(1 + \epsilon_3), \tag{14}$$

where d is one-half of the undeformed vertical aluminum ion separation. Then simply using the Pythagorean theorem, the distance between aluminum and oxide can be represented by the equation

$$r^2 = \frac{l^2}{64}\Big\{\Big(\frac{\epsilon_1^2 + 3\epsilon_2^2 + 2\epsilon_1 + 6\epsilon_2 + 4}{\sqrt{3}(1 + \epsilon_2)} + \frac{\epsilon_2^2 + 3\epsilon_1^2 + 2\epsilon_2 + 6\epsilon_1 + 4}{\sqrt{3}(1 + \epsilon_1)}\Big)^2 + \\ + \frac{64d^2}{l^2}(1 + \epsilon_3)^2\Big\}. \tag{15}$$

Neglecting terms higher than second order in the binomial expansion of eq. (15), and using the value $64d^2/l^2 = 39/2$,

$$r^2 = \frac{71}{128}l^2\Big\{1 + \frac{32}{71}\epsilon_1 + \frac{32}{71}\epsilon_2 + \frac{78}{71}\epsilon_3 - \frac{16}{71}\epsilon_1\epsilon_2 + \frac{40}{213}\epsilon_1^2 + \frac{40}{213}\epsilon_2^2 + \frac{39}{71}\epsilon_3^2\Big\}. \tag{16}$$

In the comparison of the measured value $l/r_0 = 1.316$ ($l = 2.52 \pm 0.002$Å from table I and $r_0 = 1.915$Å from table IV) with the calculated value $\sqrt{128/71}(= 1.342)$, the deviation is about 2%. This result is better than the previous equidistance approximation [6]. Finally, we get

$$r = r_0\epsilon, \tag{17}$$

where $\epsilon = \{1 + \frac{32}{71}\epsilon_1 + \frac{32}{71}\epsilon_2 + \frac{78}{71}\epsilon_3 - \frac{16}{71}\epsilon_1\epsilon_2 + \frac{40}{213}\epsilon_1^2 + \frac{40}{213}\epsilon_2^2 + \frac{39}{71}\epsilon_3^2\}^{1/2}$.

6˙2. *Pressure.* – Using hexagonal symmetry and measured values of Gieske and Barsch [3] presented in table III, the pressure-strain relations are

$$\begin{aligned} \epsilon_1 &= -(S_{11} + S_{12} + S_{13})P = -1.273 \times 10^{-13}P = -S_1P, \\ \epsilon_2 &= -(S_{11} + S_{12} + S_{13})P = -1.273 \times 10^{-13}P = -S_1P, \text{ and} \\ \epsilon_3 &= -(2S_{13} + S_{33})P = -1.414 \times 10^{-13}P = -S_3P. \end{aligned} \tag{18}$$

7. – Determination of lattice parameters

In this section an alternative form of eq. (4) around the equilibrium,

$$\phi(r) = C\left\{-r_0^2 r^{-1} + \rho\exp\left[\frac{r_0 - r}{\rho}\right]\right\}, \tag{19}$$

will be used, where $C = N\alpha^2e^2A/V_cr_0^2$ ($= 3.7078 \times 10^{20}$ erg/cm^4).

7˙1. *Lattice parameter from bulk modulus*. – From the definition of the bulk modulus,

$$K^s = -V\left(\frac{\partial P}{\partial V}\right)_s, \tag{20}$$

and thermodynamic identity for an adiabatic process,

$$\mathrm{d}U = -P\mathrm{d}V, \tag{21}$$

we get

$$K^s = V\left(\frac{\partial^2 U}{\partial V^2}\right)_s. \tag{22}$$

In our case, $U = nV_c\phi$, where n is the number of unit cells contained in a volume V and ϕ is the lattice energy density given in eq. (19). We take $n = 1$, then V_c is the volume at equilibrium. With these, the adiabatic bulk modulus becomes

$$K^s = VV_c\left(\frac{\partial^2 \phi}{\partial V^2}\right)_s. \tag{23}$$

The volume V can be parameterized by r as

$$V = V_c\left(\frac{r}{r_0}\right)^3. \tag{24}$$

Hence, the derivative with respect to V, $\partial/\partial V$, can be substituted by $(r_0^3/3V_c r^2)(\partial/\partial r)$, and eq. (23) becomes

$$K^s = \frac{r_0^3}{9} r\left\{\frac{\partial}{\partial r}\left(\frac{1}{r^2}\frac{\partial \phi}{\partial r}\right)\right\}_s. \tag{25}$$

Substituting eq. (19) into eq. (25), we get

$$K^s = \frac{Cr_0^3}{9}\left\{\left(\frac{2}{r^2} + \frac{1}{9r}\right)\exp\left[\frac{r_0 - r}{\rho} - \frac{4r_0^2}{r^4}\right]\right\}. \tag{26}$$

Substituting $r = r_0$ in eq. (26), we get

$$K_0^s = \frac{Cr_0^2}{9}\left\{\frac{1}{\rho} - \frac{2}{r_0}\right\}. \tag{27}$$

Using experimental results of Gieske and Barsch [3], we can estimate

$$\rho = 3.667 \times 10^{-9}\ (\mathrm{cm}). \tag{28}$$

7˙2. *Lattice parameter from* C_{33}. – From eq. (7), C_{33} becomes

$$C_{33} = \left.\frac{\partial^2 \phi}{\partial \epsilon_3^2}\right|_{\epsilon_3=0}.$$

Using the strain nearest-neighbor separation relation of eq. (17) and simply employing the chain rule, C_{33} becomes

$$C_{33} = \left(\frac{39}{71}\right)^2 C r_0^2 \left\{\frac{1}{\rho} - \frac{2}{r_0}\right\}. \tag{29}$$

Using experimental results of Gieske and Barsch [3], we can estimate

$$\rho = 4.410 \times 10^{-9} \text{ (cm)}. \tag{30}$$

This value differs from the value estimated from the bulk modulus data. The difference is about 20%. Both values will be used to predict the pressure derivatives of the bulk modulus, K^s, and the elastic stiffness modulus, C_{33}. We also use both values to predict the strain derivatives of the elastic stiffness modulus.

8. – Prediction of higher-order elastic properties

8˙1. *Pressure derivatives of bulk modulus*. – The bulk modulus as a function of pressure can be obtained from eq. (26) with the help of eqs. (16) and (18). Its first derivative is

$$\begin{aligned}\left.\frac{\partial K^s}{\partial P}\right|_{\substack{p=0\\ r=r_0}} &= -\frac{C r_0}{9 \times 71}(32S_1 + 39S_3)\{18 - (r_0/\rho)^2 - 6(r_0/\rho)\} \\ &= \begin{cases} 4.326, & \text{for} \quad \rho = 3.667 \times 10^{-9} \text{ cm} \\ 2.868, & \text{for} \quad \rho = 4.410 \times 10^{-9} \text{ cm}. \end{cases}\end{aligned} \tag{31}$$

The value for $\rho = 3.667 \times 10^{-9}$ (cm) which is determined from the bulk modulus is quite consistent with the measured value of Gieske and Barsch [3], $\partial K^s/\partial P = 4.32$. The second pressure derivative of bulk modulus becomes

$$\begin{aligned}&\left.\frac{\partial^2 K^s}{\partial P^2}\right|_{\substack{p=0\\ r=r_0}} = \\ &= \frac{C r_0}{9 \times 71}\Big[\frac{1}{71}(32S_1 + 39S_3)^2\{-182 + (r_0/\rho)^3 + 11(r_0/\rho)^2 + 46(r_0/\rho)\} + \\ &+\Big(\frac{32}{3}S_1^2 + 39S_3^2\Big)\{18 - (r_0/\rho)^2 - 6(r_0/\rho)\}\Big] = \\ &= \begin{cases} 6.773 \times 10^{-12} \text{ (cm}^2\text{/dyne)}, & \text{for} \quad \rho = 3.667 \times 10^{-9} \text{ cm} \\ 4.134 \times 10^{-12} \text{ (cm}^2\text{/dyne)}, & \text{for} \quad \rho = 4.410 \times 10^{-9} \text{ cm}. \end{cases}\end{aligned} \tag{32}$$

8˙2. *Pressure derivatives of* C_{33}. – The elastic stiffness modulus, C_{33}, as a function of pressure can be obtained from eq. (7) with the help of eqs. (16), (18), and (19). Its first pressure derivative is

$$\begin{aligned}(33)\qquad \left.\frac{\partial C_{33}}{\partial P}\right|_{\substack{p=0\\ r=r_0}} &= -\frac{39}{71}C\Big[\frac{78}{71}S_3(r_0^2/\rho - 2r_0) + \\ &+(32S_1+39S_3)\Big\{\frac{39}{71^2}(12r_0 - r_0^3/\rho^2 - 3r_0^2/\rho) + \frac{1}{71}(r_0^3/\rho - 2r_0^2)\Big\}\Big] \\ &= \begin{cases} 6.998, & \text{for} \quad \rho = 3.667\times 10^{-9}\ \text{cm} \\ 4.334, & \text{for} \quad \rho = 4.410\times 10^{-9}\ \text{cm}. \end{cases}\end{aligned}$$

The value for $\rho = 4.410\times 10^{-9}$ cm which is determined from C_{33} is closer to the measured value of Gieske and Barsch [3], $\partial C_{33}/\partial P = 5.00$, than the other. The deviation is about 13%. The second pressure derivative of C_{33} becomes

$$\begin{aligned}(34)\quad &\left.\frac{\partial^2 C_{33}}{\partial P^2}\right|_{\substack{p=0\\ r=r_0}} = \\ &= \frac{2\times 39^2}{71^2}CS_3\left\{S_3(-2r_0 + r_0^2/\rho) + \frac{1}{71}(32S_1+39S_3)(r_0 - 3r_0^2/\rho - r_0^3/\rho^2)\right\} - \\ &-\frac{39}{71}C\left(\frac{32}{3}S_1^2 + 39S_3^2\right)\left\{\frac{39}{71}(12r_0 - 3r_0^2/\rho - r_0^3/\rho^2) - 2r_0^2 + r_0^3/\rho\right\} + \\ &+\frac{39}{71^3}C(32S_1+39S_3)\Big[78S_3(12r_0 - 3r_0^2/\rho - r_0^3/\rho^2) + \\ &+(32S_1+39S_3)\Big\{\frac{39}{71}(-90r_0 + 15r_0^2/\rho + 6r_0^3/\rho^2 + r_0^4/\rho^3) + (10r_0^2 - 2r_0^3/\rho - r_0^4/\rho^2)\Big\}\Big] = \\ &= \begin{cases} 6.985\times 10^{-11}\ (\text{cm}^2/\text{dyne}), & \text{for} \quad \rho = 3.667\times 10^{-9}\ \text{cm} \\ 4.418\times 10^{-11}\ (\text{cm}^2/\text{dyne}), & \text{for} \quad \rho = 4.410\times 10^{-9}\ \text{cm}. \end{cases}\end{aligned}$$

8˙3. *Strain derivatives of* C_{33}. – In the case of uniaxial stresses, the strain derivative of the elastic moduli such as $-(1/C_{33})(\partial C_{33}/\partial\epsilon_3)$ and $(1/C_{33}^2)(\partial^2 C_{33}/\partial\epsilon_3^2)$ which correspond to $\partial C_{33}/\partial P$ and $\partial^2 C_{33}/\partial P^2$, respectively, in the hydrostatic case are commonly considered. The ϵ_3 dependence of C_{33} can be derived from eqs. (7), (16), and (19). From this, we get

$$\begin{aligned}(35)\quad -\frac{1}{C_{33}}\left.\frac{\partial C_{33}}{\partial\epsilon_3}\right|_{\substack{\epsilon_3=0\\ r=r_0}} &= -\frac{39^2}{71^2}\frac{C}{C_{33}}\left\{3(-2r_0 + r_0^2/\rho) + \frac{39}{71}(12r_0 - 3r_0^2/\rho - r_0^3/\rho^2)\right\} = \\ &= \begin{cases} 3.127, & \text{for} \quad \rho = 3.667\times 10^{-9}\ \text{cm} \\ 1.663, & \text{for} \quad \rho = 4.410\times 10^{-9}\ \text{cm}. \end{cases}\end{aligned}$$

Both of these results are further from the measured value 5.00 than the results in eq. (33). Finally, $(1/C_{33}^2)(\partial^2 C_{33}/\partial\epsilon_3^2)$ becomes

$$\begin{aligned}(36)\quad \frac{1}{C_{33}^2}\frac{\partial^2 C_{33}}{\partial\epsilon_3^2} &= \frac{39^2}{71^2}\frac{C}{C_{33}^2}\Bigg[-6r_0 + 3r_0^2/\rho + \frac{117}{71}(12r_0 - 3r_0^2/\rho - r_0^3/\rho^2) + \\ &+\frac{39}{71}\left\{36r_0 - 9r_0^2/\rho - 3r_0^3/\rho^2 + \frac{39}{71}(-90r_0 + 15r_0^2/\rho + 6r_0^3/\rho^2 + r_0^4/\rho^3)\right\}\Bigg] =\end{aligned}$$

TABLE V. – *List of predicted values of higher-order elastic properties of corundum in CGS units: Measured values are relisted for comparison.*

	Measured value of Gieske and Barsch [3]	Computed from bulk modulus	Computed from C_{33}
Lattice parameter (ρ)	–	3.667×10^{-9}	4.410×10^{-9}
$\partial K^s/\partial P$	4.32	4.326	2.867
$\partial^2 K^s/\partial P^2$	–	6.773×10^{-12}	4.134×10^{-12}
$\partial C_{33}/\partial P$	5.00	6.998	4.334
$-\frac{1}{C_{33}}(\partial C_{33}/\partial \epsilon_3)$	–	3.127	1.663
$\partial^2 C_{33}/\partial P^2$	–	6.985×10^{-11}	4.418×10^{-11}
$\frac{1}{C_{33}^2}(\partial^2 C_{33}/\partial \epsilon_3^2)$	–	-2.958×10^{-13}	-6.092×10^{-13}

$$= \begin{cases} -2.958 \times 10^{-13}\ (\mathrm{cm}^2/\mathrm{dyne}), & \text{for} \quad \rho = 3.667 \times 10^{-9}\ \mathrm{cm} \\ -6.092 \times 10^{-13}\ (\mathrm{cm}^2/\mathrm{dyne}), & \text{for} \quad \rho = 4.410 \times 10^{-9}\ \mathrm{cm}. \end{cases}$$

Those three predicted second derivatives are the major results of this work. They can be used in extrapolations of $K^s(P)$, $C_{33}(P)$, and $C_{33}(\epsilon_3)$.

9. – Conclusions and discussions

A static rigid-ion lattice model for corundum, utilizing the exponential-type repulsive potential for the nearest neighbors, was developed. The lattice parameters were determined from measured data of bulk modulus and C_{33}. Using these lattice parameters, theoretical higher-order elastic properties were computed. The results are summarized in table V. The predicted value of $\partial K^s/\partial P$ using the lattice parameter, ρ, determined from K^s is consistent with the measured value. However, the predicted value of $\partial C_{33}/\partial P$ using the lattice parameter ρ determined from C_{33} is closer to the measured value than that determined from K^s. The deviation of each result does not exceed 33%. The predicted second pressure derivatives of K^s and C_{33} seem to be reliable. $-(1/C_{33})(\partial C_{33}/\partial \epsilon_3)$ and $(1/C_{33}^2)(\partial C_{33}^2/\partial \epsilon_3^2)$ are quite different from the measured and predicted values of $\partial C_{33}/\partial P$ and $\partial^2 C_{33}/\partial P^2$, respectively. The differences between predicted values and measured values may come from

– the idealized model (It is not a perfect hexagonal closed-packed structure, and the distances between aluminum and oxygen ions are not uniform.),

– neglecting the covalent bonding character (The model considered only Coulomb's force and central repulsive forces.), and

– neglecting the next nearest neighbors' effects (The model considered only the nearest neighbors' repulsive forces.).

An interesting aspect of our results is that the predicted second pressure derivatives of K^s and C_{33} are positive. These differ from those of cubic structured oxide minerals which have negative values of $\partial^2 K^s/\partial P^2$ and $\partial^2 C_{33}/\partial P^2$ [10]. Further investigation of a more complicated model including next nearest neighbors' effects would be of great interest.

* * *

This work was funded by the Korea Meteorological Administration Research and Development Program under Grant CATER 2006-5206. The authors wish to thank Prof. E. K. Graham, the Pennsylvania State University, and anonymous reviewer for their suggestions and critical reviews.

REFERENCES

[1] Pauling L. and Hendricks S. B., *J. Am. Chem. Soc.*, **47** (1925) 781.
[2] Newnham R. E. and De Haan Y. M., *Z. Kristallogr.*, **117** (1962) 235.
[3] Gieske J. H. and Barsch G. R., *Phys. Status Solidi*, **29** (1968) 121.
[4] Thurston R. N., *J. Acoust. Soc. Am.*, **41** (1967) 1093.
[5] Schmaeling V., *Z. Phys.*, **47** (1928) 723.
[6] Sherman J., *Chem. Rev.*, **11** (1932) 93.
[7] Born M. and Lande A., *Verh. D. Phys. Ges.*, **20** (1918) 210 recited from Hϕjendahl K., *Det. Kgl. Danske Vid. Selsk.*, **16**, Sec. 2 (1938).
[8] Born M. and Mayer J. E., *Z. Phys.*, **75** (1932) 1.
[9] Clark S. P., Jr., *Conversion Factors, Numerical Constants, Atomic Constants, in Handbook of Physical Constants*, edited by Clark S. P., Jr., *Geol. Soc. Am.*, Memoir 97 (1966) 580.
[10] Prosser P. M. and Graham E. K., *Phys. Earth Planet. Int.*, **34** (1984) 85.